phological change to afford the normal bilayer membranes upon incubation with the bilayer aggregates composed of ionic peptide lipids $N^+C_5Ala2C_n$ and $(SO_3^-)C_5Ala2C_n$. The transfer of the ionic lipid molecules involved in the bilayer membranes to the QC_5Ala2C_n aggregates occurs through the intervening aqueous phase. The ionic lipid molecules invaded into the aggregates of QC_5Ala2C_n may act to break down the strong intermolecular

hydrogen-bonding interaction between the quinoyl moieties of the nonionic lipids and lead to the formation of the normal bilayer membranes.

Absorption and MCD Spectral Studies of the Decaammine(μ-dinitrogen-N',N')diosmium(5+) Mixed-Valence Ion

Lucjan Dubicki,[†] **James Ferguson,**[*†] **Elmars R. Krausz,**[†] **Peter A. Lay,**[†] **Marcel Maeder,**[†] **Roy H. Magnuson,**[‡] **and Henry Taube**[*‡]

Contribution from the Research School of Chemistry, Australian National University, Canberra, A.C.T., 2601, Australia, and the Department of Chemistry, Stanford University, Stanford, California 94305. Received May 22, 1984

Abstract: The red and near-infrared absorption and MCD spectra of the title compound have been measured over a range of temperature in KCl disks and poly(vinyl alcohol) (PVA). The two most intense bands, near 5500 and 14 300 cm^{-1}, have MCD C terms of opposite sign. A "single-ion" band whose energy is determined dominantly by spin–orbit coupling on osmium(III) occurs at 4700 cm^{-1}. Two other weaker absorptions appear near 8200 and 16 000 cm^{-1}. All of these bands have been interpreted by using a simple coupled chromophore model in which degeneracies are removed by a one-electron-transfer integral that models π bonding via the dinitrogen bridging ligand, between the d_{xz} and d_{yz} orbitals on each metal ion. Also essential to this model is the inclusion of both spin–orbit coupling on the metal centers and the tetragonal field due to the dinitrogen bridge via an effective Hamiltonian treatment. Allowed electric dipole absorption intensities have been formulated in terms of effective electric dipole transition matrix elements. These are determined by the odd-parity components associated with the C_{4v} site symmetry of each metal center within the dimer. The model is consistent with a qualitative MO description that includes spin–orbit coupling.

Although the first dinitrogen-bridged complex, $[(NH_3)_5RuN_2Ru(NH_3)_5]^{4+}$, was reported in 1968,[1] spectroscopic properties of the corresponding mixed-valence (5+) ion were reported only very recently along with the Os analogue.[2] Apart from the interest in these complexes from the viewpoint of N_2 fixation,[2] the osmium complex was the first example of a stable mixed-valence ion that has both high symmetry (D_{4h}) and more than one atom in the bridge between the two metal centers. Its stability and symmetry are, of course, most attractive for spectroscopic measurements and allow a direct comparison with the much studied pyrazine-bridged complexes having D_{2h} symmetry.[3] Studies of these latter complexes have been seminal in the formation of several models of mixed-valence "delocalization",[4] but the situation is not clearly resolved even in the most recent calculations.[5]

A simple MO scheme without spin–orbit coupling[2] cannot give a quantitative description of the observed spectra. We have used an effective Hamiltonian model,[6] essentially a valence-bond method, that is more convenient for the calculation of transition intensities and for the inclusion of spin–orbit coupling. This paper reports the absorption and MCD of the title compound, together with a theoretical analysis.

Octahedral Os(III), having a hole in the t_2 shell, has only a single term of T_2 symmetry which is also well separated from others associated with other electronic configurations (e_g and charge transfer) so that an effective Hamiltonian model is very well suited for the analysis of spin–orbit and low-symmetry effects in the monomer case. The same approach can be used for symmetric dimers by including an interion coupling term in the effective Hamiltonian. We have developed such a model[7] for the well-known mixed-valence ruthenium Creutz–Taube dimer and the corresponding osmium ion.[8] Whereas the metal ions in the pyrazine dimer have C_{2v} symmetry, so that the μ-dinitrogendiosmium ion is C_{4v} and the symmetric dimer has D_{4h} symmetry.

This change to 4-fold symmetry produces significant differences in the calculated energy level patterns which are borne out by analyses of the absorption spectrum and the corresponding MCD of the title compound.

MCD Spectroscopy

MCD spectroscopy[9] is a very powerful method in the assignment of absorption spectra of transition-metal-ion complexes. It has been used to analyze the near-infrared spectra of pentaamine complexes of Os(III) with π-bonding ligands.[10]

MCD spectroscopy has recently been introduced to the study of mixed-valence compounds.[7,11] Mixed-valence compounds most often have dominant linear (interion) polarization of absorption. This is easily understood as intensity arises fundamentally from the transfer of an electron from one metal center to the other, even in the case of strongly coupled symmetric systems! In the recent extensive MO calculations of Ondrechen et al.,[5] the characteristic transition in the Creutz–Taube complex is reaffirmed

(1) Harrison, D. E.; Weisberger, E.; Taube, H. *Science (Washington, D.C.)* **1968**, *159*, 320–322.

(2) Richardson, D. E.; Sen, J. P.; Buhr, J. D.; Taube, H. *Inorg. Chem.* **1982**, *21*, 3136–3140.

(3) Creutz, C. *Prog. Inorg. Chem.* **1983**, *30*, 1–73.

(4) Brown, D. M., Ed. "Mixed-Valence Compounds"; Reidel: Dordrecht, Holland, 1980.

(5) Ondrechen, M. J.; Ellis, D. E.; Ratner, M. A. *Chem. Phys. Lett.* **1984**, *109*, 50–55.

(6) Sugano, S.; Tanabe, Y.; Kamimura, H. "Multiplets of Transition-Metal Ions in Crystals"; Academic Press: New York, 1970.

(7) Dubicki, L.; Ferguson, J.; Krausz, E. R. *J. Am. Chem. Soc.* **1985**, *107*, 179–182.

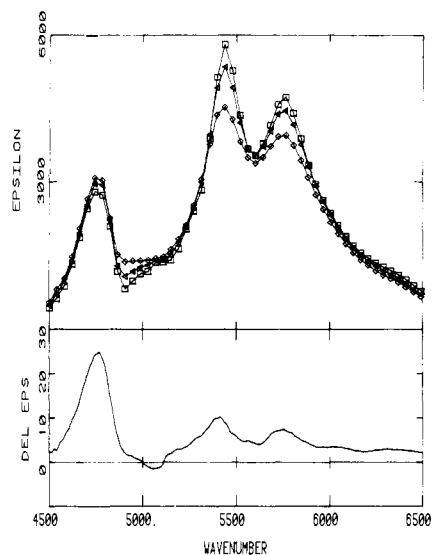(8) Magnuson, R. H.; Lay, P. A.; Taube, H. *J. Am. Chem. Soc.* **1983**, *105*, 2507–2509.

(9) Piepho, S. B.; Schatz, P. N. "Group Theory in Spectroscopy"; Wiley: New York, 1983.

(10) Dubicki, L.; Ferguson, J.; Krausz, E. R.; Lay, P. A.; Maeder, M.; Taube, H. *J. Phys. Chem.* **1984**, *88*, 3940–3941.

(11) Krausz, E. R.; Ludi, A. *Inorg. Chem.*, in press.

[†] Australian National University.
[‡] Stanford University.

Figure 1. Electronic absorption spectrum of decaammine(μ-dinitrogen-N',N')diosmium(5+) in PVA at 8 K ($\diamond$), 130 K ($\triangle$), and 220 K ($\square$) (upper panel) and its MCD (5.5 K) (lower panel).

Figure 2. Electronic absorption spectrum of decaammine(μ-dinitrogen-N',N')diosmium(5+) in PVA at 8 K ($\square$) and 300 K ($\star$) (upper panel) and its MCD (5.5 K) (lower panel).

as being basically between symmetric and antisymmetric combinations of metal-centered orbitals. The transition dipole matrix element is again simply $\langle$Ru(II)|er|Ru(III)$\rangle$.

The MCD of a purely linearly polarized transition is necessarily zero, but MCD may arise from an interference process between the linearly polarized (z) two-centered process described and a (weaker) single-centered process that has x and/or y polarization. The latter is called a single-ion process. For a system of randomly oriented species as occurs in solutions or glasses, the interference MCD process is observed for the dimers that are oriented with the magnetic field transverse to the interion direction.[12]

Experimental Section

Measurement of MCD requires an optically isotropic propagation direction in the sample medium. We used two mediums, either pressed KCl disks or foils of poly(vinyl alcohol) (PVA) made by evaporation of concentrated (acidified) water solutions of PVA and the dissolved complex ion. In general we have found that the PVA foils scatter less but generally display broader absorption bands and have characteristic absorptions around 4000 cm^{-1}. Nonpolar materials have limited solubilities in PVA. The spectra obtained from materials pressed in KCl disks tend to have nonlinear absorption intensities and can contain spectral artifacts associated with reflectance from the small crystals dispersed in the KCl. The availability of these two isotropic mediums helps to provide important checks of both MCD and absorption features.

The MCD apparatus has been described earlier[13] for photomultiplier detection. For the near-infrared region, the detector system used an InAs or InSb device. A detailed description of the apparatus is given elsewhere.[11]

[(NH$_3$)$_5$OsN$_2$Os(NH$_3$)$_5$]Cl$_5$·H$_2$O was prepared by improved methods to those reported previously.[2]

Results

Details of the room-temperature absorption spectrum of the compound have been given previously.[2] We concentrate here on the temperature dependence of the absorption spectrum between 300 and about 10 K. As for the pyrazine dimer,[8] there are three absorption regions in the near-infrared and the red spectral regions. Closer study reveals significant differences between these two sets of mixed-valence-ion spectra. We consider first the lowest energy band group which contains three main components (bands at 4760, 5440, and 5750 cm^{-1}).

Measurement of the temperature dependence of the absorption
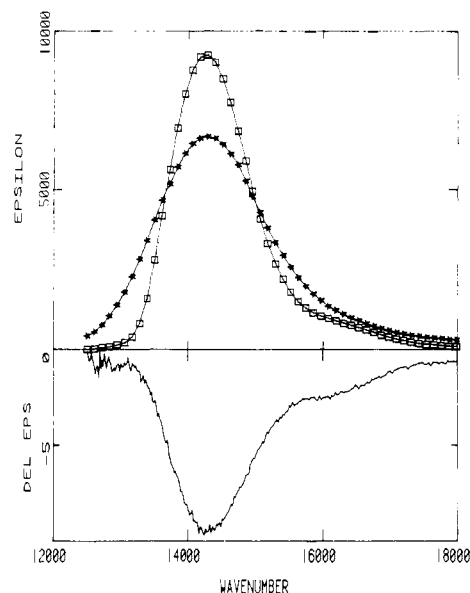
spectrum in the lowest energy region establishes that the temperature dependence of the intensity of the 4760-cm^{-1} component is opposite to that of the other two. This is illustrated in Figure 1 where it can be seen that the intensity of the lowest energy component decreases on lowering the temperature. This behavior is not consistent with a charge-transfer mechanism, in contrast to the other two bands which show the expected intensity increase on cooling. The 4760-cm^{-1} band therefore appears to be electronically forbidden and the band should be seen as a false origin, i.e., a non-totally symmetric vibration coupled to a forbidden electronic origin. There is also another much weaker band at 5100 cm^{-1} which shows the same temperature behavior and is therefore another false origin.

Consideration of the MCD, included in Figure 1, emphasizes the spectral differences evident from the effect of change of temperature. The lowest energy component shows a larger signal than the remainder of the band group, again indicating a different mechanism for the absorption of light to this state. In addition the second false origin, near 5100 cm^{-1}, has MCD with the opposite sign (negative). The temperature dependence of the MCD showed it to be dominated by C terms[9] and thus the MCD arises from the difference in population between the Zeeman levels in the ground state.

We turn next to the highest energy band in the red spectral region. In this case decrease of temperature reveals a weak higher energy band at 16 000 cm^{-1}, and both are shown in Figure 2 along with their MCD, which are again C terms.

A third comparatively weak absorption band is observed at an energy of 8200 cm^{-1} between the two main regions of absorption, while there are a few very weak absorption bands on either side of it. The MCD recorded in this region shows a negative C term.

Effective Hamiltonian for the Dimer

Our theoretical analysis involves a description of the (a,b) dimer in terms of simple product functions $d_a^6 d_b^5$ and $d_a^5 d_b^6$, which interact via a one-electron transfer integral. The cubic axes (x, y, z) on both centers are matched with the pair axes (X, Y, Z), where Z lies along the Os–Os direction. The transfer integral then arises from the interaction between the π orbitals on the bridging ligand and the d_{xz} and d_{yz} orbitals of the metal ions. The effective Hamiltonian for, say, the $d_a^6 d_b^5$ configuration is

$$\mathcal{H}_{\text{eff}} = \Delta(L_z^2 - \tfrac{2}{3}) - \lambda LS$$

Δ is the tetragonal splitting parameter $E(d_{xy}) - E(d_{xz})$ and λ is the spin–orbit coupling parameter, a positive quantity. We use

(12) Dubicki, L.; Ferguson, J. *Chem. Phys. Lett.* **1984**, *109*, 128–131.
(13) Ferguson, J.; Krausz, E. R.; Guggenheim, H. J. *Mol. Phys.* **1974**, *27*, 577–591.

Table I. Eigenstates and Eigenvalues for the D_{4h} Mixed-Valence Dimer[a]

Eigenstates[b]

$$\Phi_{1\mp}^{B} = [(d_a^6 \pm 1/2 X_{\pm b}) + (\pm 1/2 X_{\pm a} d_b^6)]/2^{1/2}$$

$$\Phi_{2\mp}^{B} = \cos\Theta_B[(d_a^6 \mp 1/2 X_{0b}) + (\mp 1/2 X_{0a} d_b^6)]/2^{1/2} + \sin$$
$$\Theta_B[(d_a^6 \pm 1/2 X_{\mp b}) + (\pm 1/2 X_{\mp a} d_b^6)]/2^{1/2}$$

$$\Phi_{3\mp}^{B} = \sin\Theta_B[(d_a^6 \mp 1/2 X_{0b}) + (\mp 1/2 X_{0a} d_b^6)]/2^{1/2} - \cos$$
$$\Theta_B[(d_a^6 \pm 1/2 X_{\mp b}) + (\pm 1/2 X_{\mp a} d_b^6)]/2^{1/2}$$

Eigenvalues (Units of λ)

$$E_1^B = -2W/3 + {}^1/_2$$
$$E_2^B = -2W/3 - 2\Delta_B/3 + \tan\Theta_B/2^{1/2}$$
$$E_3^B = -2W/3 - 2\Delta_B/3 - \cot\Theta_B/2^{1/2}$$
$$E_1^A = 2W/3 + \Delta_A/3 + {}^1/_2$$
$$E_2^A = 2W/3 - 2\Delta_A/3 + \tan\Theta_A/2^{1/2}$$
$$E_3^A = 2W/3 - 2\Delta_A/3 - \cot\Theta_A/2^{1/2}$$

[a] $\tan 2\Theta_B = 2^{1/2}/({}^1/_2 - \Delta_B)$; $\tan 2\Theta_A = 2^{1/2}/({}^1/_2 - \Delta_A)$; $\Delta_B = \Delta - W$; $\Delta_A = \Delta + W$. Δ and W are in units of λ. [b] For A functions replace the + combination by – and Θ_B by Θ_A.

complex tetragonal orbitals $|x_\pm\rangle = \mp(d_{yz} \pm id_{xz})/2^{1/2}$ and $|x_0\rangle = d_{xy}$. The corresponding five-electron functions, $|M_S M\rangle$, are given elsewhere.[7] The dimer bases are $|M_S M_a d_b^6\rangle$ and $|d_a^6 M_S M_b\rangle$. The elements of the interior interaction (transfer integral) are restricted to

$$\langle d_a^6 M_S X_{\pm b}| \mathcal{H}_{ab}| M_S X_{\pm a} d_b^6\rangle = -W$$

corresponding to the following matrix elements between orbitals

$$\langle d_{(yz)a}| \mathcal{H}_{ab}| d_{(yz)b}\rangle = \langle d_{(xz)a}| \mathcal{H}_{ab}| d_{(xz)b}\rangle = W$$

The transfer integral between d_{xy} orbitals is neglected because they are orthogonal to the valence orbitals of the bridging ligand.

The dimer eigenstates and eigenvalues are given in Table I. They fall into two sets, B and A, which are even and odd, respectively, under inversion symmetry in the group D_{4h}. The parameters Δ and W are related to orbital energies (E) of a simple MO model,

$$W = {}^1/_2(E(e_g) - E(e_u))$$

$$\Delta = {}^1/_2(E(b_{1u}) + E(b_{2g}) - E(e_g) - E(e_u))$$

where e_g, b_{2g}, b_{1u}, and e_u are molecular orbitals with predominantly metal t_{2g} character. The b_{2g} and b_{1u} orbitals are nonbonding and assumed to be degenerate. This degeneracy may be lifted by the presence of a weak δ interaction. The $e_g \approx (d_{(xz)a} + d_{(xz)b})/2^{1/2}$ and $(d_{(yz)a} + d_{(yz)b})/2^{1/2}$ orbitals are stabilized by π back-bonding with the $\pi^* e_g$ orbitals of the bridging ligand. The e_u orbitals are destabilized by π interaction with the ligand πe_u orbitals and contain three electrons including the unpaired electron. W is negative in our terminology, and since the back-bonding is stronger than the forward bonding[16] in this material, Δ by the above definition is positive. Thus Φ_3^A in Table I becomes the ground doublet.
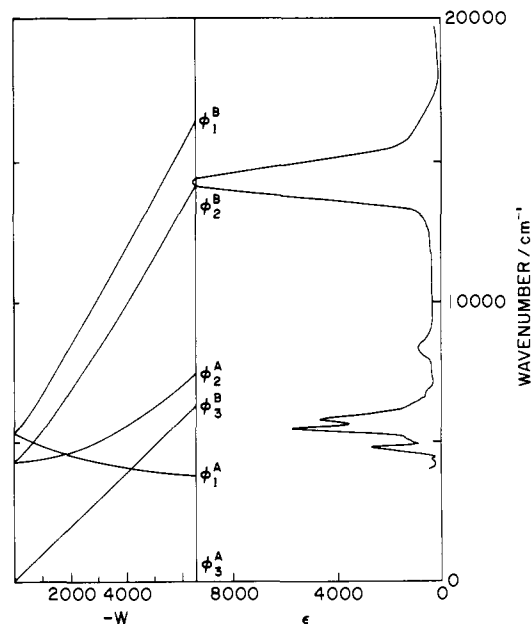
Our approach is similar to Anderson's superexchange theory for pairs of insulator ions.[14,15] The basis orbitals, d_{xz}, d_{yz}, and d_{xy}, should be regarded as orthogonal atomic orbitals, d^0. For example, a more explicit form for the d_{xz} orbital is

$$d_{(xz)a}^0 \approx d_{(xz)a} - \lambda(\pi e_u) + \gamma(\pi^* e_g)$$

$$d_{(xz)b}^0 \approx d_{(xz)b} + \lambda(\pi e_u) + \gamma(\pi^* e_g)$$

where λ and γ are positive mixing coefficients.

Our analysis of the absorption and MCD spectra requires a consideration of the mechanism of absorption of light. The observed intensities are too large to include significant magnetic dipole contributions, so they must be electric dipole in nature. Electric dipole processes can be either vibronically induced, breaking down the Laporte restriction, or allowed by the static

(14) Anderson, P. W. *Solid State Phys.* **1963**, *14*, 99.

(15) Gondaira, K.; Tanabe, Y. *J. Phys. Soc. Jpn.* **1966**, *21*, 1527–1548.

Figure 3. Calculated energy level scheme as a function of W for a value of $\Delta = 1800$ cm^{-1} and $\lambda = 3000$ cm^{-1}. The observed 8 K absorption spectrum is shown on the right-hand side.

Table II. Transition Electric Dipole Strengths for D_{4h} Pairs and MCD (Linear Limit) $\bar{C}_0$ Terms[a]

Dipole Strengths

$\Phi_3^B \leftarrow \Phi_3^A$	$[\sin\Theta_A \cos\Theta_B(a - 2b) - \cos\Theta_A \sin\Theta_B(a + b)]^2$
$\Phi_3^B \leftarrow \Phi_3^A$	$[\sin\Theta_A \sin\Theta_B(a - 2b) + \cos\Theta_A \cos\Theta_B(a + b)]^2$

$D^X = D^Y$

$\Phi_1^B \leftarrow \Phi_3^A$	$c^2 \sin^2\Theta_A/2$
$\Phi_2^B \leftarrow \Phi_3^A$	$c^2 \cos^2(\Theta_A - \Theta_B)/2$
$\Phi_3^B \leftarrow \Phi_3^A$	$c^2 \sin^2(\Theta_A - \Theta_B)/2$

MCD (Linear Limit) $\bar{C}_0$ Terms (Spatially Averaged)

$\Phi_1^B \leftarrow \Phi_3^A$	$-(g_z \sin^2\Theta_A c^2)/6$
$\Phi_2^B \leftarrow \Phi_3^A$	$(2(2)^{1/2}g_x c(\sin\Theta_A \cos\Theta_B(a - 2b) - \cos\Theta_A \sin\Theta_B(a + b)) \cos(\Theta_A - \Theta_B) + g_z \cos^2(\Theta_A - \Theta_B)c^2)/6$
$\Phi_3^B \leftarrow \Phi_3^A$	$(-2(2)^{1/2}g_x c(\sin\Theta_A \sin\Theta_B(a - 2b) + \cos\Theta_A \cos\Theta_B(a + b)) \sin(\Theta_A - \Theta_B) + g_z \sin^2(\Theta_A - \Theta_B)c^2)/6$

[a] The first-order g factors with orbital reduction parameter $k = 1$ are $g_z = -4\cos^2\Theta_A + 2\sin^2\Theta_A$, $g_x = 2^{1/2}\sin 2\Theta_A + 2\sin^2\Theta_A$, and $\tan 2\Theta_A = 2^{1/2}/({}^1/_2 - \Delta_A)$. Δ_A is units of λ.

components of the noncentrosymmetric field at each metal ion. The latter have C_{4v} site symmetry so we require the odd-parity components of C_{4v} symmetry. It is convenient to consider effective electric dipole transition matrix elements that are determined by these odd-parity components.[6] There are three reduced matrix elements: $a = -1/3\langle T_2||V(A_1)||T_2\rangle$; $b = 1/3(2^{1/2})\langle T_2||V(E)||T_2\rangle$; $c = 1/2(3^{1/2})\langle T_2||V(T_2)||T_2\rangle$. b and c are associated with single-ion z and x,y polarizations, respectively, while a represents the two-center (z) polarization.[12] The pair electric dipole intensities and the MCD C terms are given in Table II and were calculated from eq 15 in ref 12. We do not attempt to calculate vibronically induced intensities at this stage.

Analysis and Discussion

It is instructive to see how the energy levels of the dimer vary with the parameter W for a given Δ, shown in Figure 3. The magnitude of Δ is not directly determined. However, arguments relating to π back-bonding in these materials[2,16] would indicate that Δ is positive, as previously indicated. We use a value that provides reasonable agreement with experiment for a value of W which fits the highest two bands.

The first point to note about Figure 3 is the appearance of a

(16) Buhr, J.; Taube, H. *Inorg. Chem.* **1980**, *19*, 2425–2434.

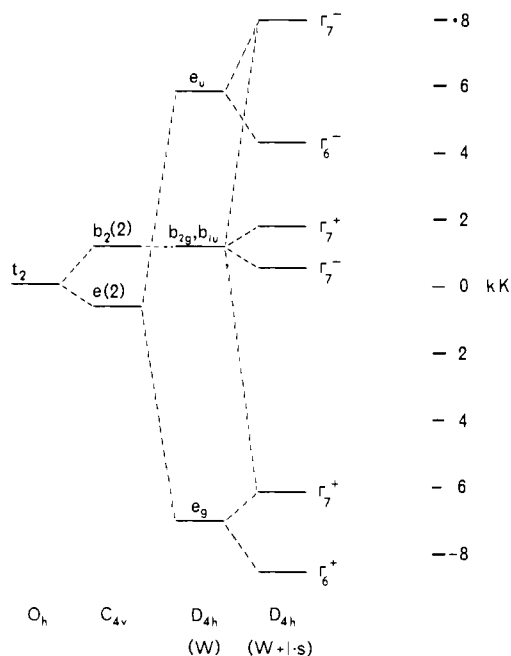**Figure 4.** One-electron orbital energy diagram for $\Delta = 1800$ cm^{-1}, $\lambda = 3000$ cm^{-1}, and $W = -6500$ cm^{-1}. The diagram has to be inverted for the five-electron states, which are denoted by Φ in Figure 3.

state (Φ_1^A) whose energy is determined primarily by the spin–orbit coupling of the d^5 configuration, and because its energy is only weakly dependent on W, the associated absorption band should be relatively sharp. Its calculated energy also lies lower than the observed position. We assign the region between 4500 and 5200 cm^{-1} to transitions to Φ_1^A which are vibrationally induced. This conclusion is substantiated by both the temperature dependence of the intensity of these bands as seen in Figure 1 and observations of the absorption spectra of deuterated materials which show a substantial shift in this region.

The remaining two components of the lowest energy band group are assigned to the second excited state (Φ_3^B). The band at 8200 cm^{-1} is assigned to the third excited state (Φ_2^A), which being parity forbidden, is only vibronically allowed. This again is substantiated by the observed temperature dependence. Finally, absorption in the red region comprises two bands separated by about 2000 cm^{-1}. The lower and more intense of these is assigned to the fourth excited state (Φ_2^B) while the weak higher energy band is assigned to the remaining excited state (Φ_1^B). Considering the simplicity of the model, the observed energies of the states are well accounted for by a value of $W = -6500$ cm^{-1}.

The proposed assignments are strongly reinforced by a consideration of the intensities of the absorption and MCD spectra. The z-polarized intensity should occur in the transitions to Φ_2^B and Φ_3^B, which should be the most intense bands, in agreement with observation. Assuming a dominant Z-polarized electron-transfer dipole, the parameter b^2 can be ignored and the theoretical ratio of intensities is sin^2 $(\Theta_A - \Theta_B)$:cos^2 $(\Theta_A - \Theta_B) = 7{:}3$ ($\Phi_2^B{:}\Phi_3^B$), in good agreement with the observed ratio 9:3. The discrepancy may be accounted for by the proximity of the higher level to ligand charge-transfer states that may leak extra intensity into the upper level preferentially.

The highest energy band, although formally allowed, should carry no Z-polarized intensity, and therefore it should be weaker than the other two bands. The remaining two weak bands (Φ_1^A and Φ_2^A) are electric dipole forbidden and may gain intensity through coupling to odd-parity vibrations.

The assignments are supported by the MCD spectra. For the two intense transitions (Φ_2^B and Φ_3^B) the MCD should be determined mainly by the transverse interference terms. From Table II we predict

$$C_0(\Phi_2^B)/C_0(\Phi_3^B) \approx$$
$$[-ac \sin 2(\Theta_A - \Theta_B)]/[ac \sin 2(\Theta_A - \Theta_B)] = -1$$

in reasonable agreement with the observed ratio –1.5. The absolute signs of the MCD intensities cannot be determined by using this parameterized approach.

The sign of the MCD associated with the transition to Φ_1^B should be positive, in contrast to its observed negative sign. Also, the theoretical dipole strength and MCD C term are both proportional to c^2 and in the limit of complete saturation $\Delta A/A = 1$, whereas the observed $\Delta A/A \approx -0.005$. The observed band intensity therefore cannot be due to the electric dipole parameter c. We note from Figure 2 that the absorption intensity does not increase on cooling, in contrast to that at 14 300 cm^{-1}, and it is therefore not a vibrational satellite of $\Phi_2^B \leftarrow \Phi_3^A$. Its behavior is consistent with the intensity coming from a vibronic coupling between the two states (Φ_1^B and Φ_2^B) so that its dipole strength and MCD C term are both vibronically induced. There is some indirect evidence to support this conclusion from a study of the near-infrared absorption and MCD of the C_{4v} pentaammine complexes Os-$(NH_3)_5X^{2+}$ (X = Cl, Br, I), presently in progress. The analogous single-ion transition has positive MCD and larger $\Delta A/A$ values, in agreement with intensity predominantly arising from the c parameter.[7]

It is important to note that the electronic parameters Δ and W depend on vibrational coordinates. In particular, the transfer integral (W) is sensitive to the separation (R) of the two metal ions. A change in R is proportional to changes in the symmetric combination mode of monomer vibrational coordinates. Hence these totally symmetric vibrations will contribute to the bandwidth of the electronic transitions. As noted by Wong and Schatz,[17] in the absence of such a dependence, involvement of the symmetric mode is strictly forbidden.

The transition energy to Φ_1^A is approximately independent of W but varies as $-W$ to Φ_3^B and $-2W$ to the Φ_2^B state. It is easy to see that for the simple case of the symmetric vibration, $Q_g = (Q_a + Q_b)/^{1/2}$, where Q_a and Q_b are coordinates in the breathing modes of a and b, respectively, and the equilibrium displacement of Q_g for the Φ_1^A state is ≈ 0 and is nonvanishing for the Φ_3^B and Φ_2^B states but twice as large for the latter. This analysis qualitatively accounts for the bandwidths observed at low temperatures, viz. $\nu_{1/2} = 190$ cm^{-1} for $\Phi_1^A \leftarrow \Phi_3^A$ (e$_u$ $\leftarrow$ e$_u$), $\Delta\nu = 320$ cm^{-1} (mean separation of the two intense bands) for $\Phi_3^B \leftarrow \Phi_3^A$ (e$_u \leftarrow$ b$_{2g}$), and $\nu_{1/2} = 1300$ cm^{-1} for $\Phi_2^B \leftarrow \Phi_3^A$ (e$_u \leftarrow$ e$_g$). The symbols in parentheses refer to the one-electron orbital jump from which the transition specified is principally derived.

The MCD spectra provide additional support for the activity of totally symmetric vibrations. The electron-transfer dipole is a static mechanism and, in transverse MCD, interferes with a static single-ion electric dipole. Within the Born–Oppenheimer (BO) approximation the Z-polarized absorption intensity and the transverse MCD intensity can be distributed only by totally symmetric vibrations. This is confirmed by the MCD of the Φ_3^B and Φ_2^B bands, which follows the absorption profile. The predominance of the electron-transfer dipole makes the line shape of the Φ_2^B and Φ_3^B bands in solution (and Z-polarized crystal) spectra relatively simple. Crystal spectra with light polarized perpendicular to Z should be less intense but rich in false origins and we have noted such behavior.

We note finally that our analysis of the electronic spectrum gives $\Theta_A \approx 17°$ (see Table I) and the first-order g factors are predicted to be $g_z \approx -3.5$ and $g_x \approx +0.9$. Preliminary EPR measurements in a glassy matrix of DMF/H$_2$O at 15 K show very broad features consistent with $|g_\parallel| \approx 3.5$ and $|g_\perp| \approx 1.5$.

Conclusions

The title compound is undoubtedly a delocalized mixed-valence pair, and the main spectroscopic features of the ($^1A_1 \times {}^2T_2$) multiplet can be explained within the BO approximation. Most of the intensity arises from the electron-transfer dipole. However,

(17) Wong, K. Y.; Schatz, P. N. In "Mechanistic Aspects of Inorganic Reactions"; Rorabacher, D. B., Endicott, J. F., Eds.; American Chemical Society: Washington, DC, 1982; ACS Symp. Ser. No. 198.

the vibronically induced electric dipole (Herzberg–Teller coupling) appears to dominate the parity-forbidden transitions *as well as* the transitions allowed through a static single-ion mechanism. Spin–orbit coupling significantly perturbs the electronic energy levels and redistributes the Z-polarized intensity. For example, the $\Phi_3^B \leftarrow \Phi_3^A$ transition is nominally XY allowed as a one-electron $e_u \leftarrow b_{2g}$ excitation but is in fact predominantly Z polarized.

The same theoretical model has been applied to the Creutz–Taube ion.[7] Unfortunately, in that case only one electronic state of the $(^1A_1 \times {}^2T_2)$ multiplet has been clearly identified. Furthermore, the MCD does not follow the absorption profile as closely as in the present case. It seems likely that the vibronically induced electric dipole gives a larger contribution in the Creutz–Taube ion. In the absence of a detailed analysis of the vibronically induced contribution to the absorption and MCD intensities there seems to be no compelling reason to invoke the breakdown of the BO approximation in the Creutz–Taube ion.

A more sensitive test for the breakdown of the BO approximation in both the title and Creutz–Taube complex would be the detection of the so-called "tunneling" transitions in the IR region. This phenomenon is beyond the scope of our current model. The PKS model[4,17] extended to include spin–orbit coupling and all the electronic states of the $^2T_2$ multiplet would have application.

Communications to the Editor

Homoleptic Carbene Complexes. 3. Hexakis(oxazolidin-2-ylidene)cobalt(III) and -rhodium(III)[1]

Ulrike Plaia, Heribert Stolzenberg, and Wolf P. Fehlhammer*

*Institut für Anorganische und Analytische Chemie der Freien Universität Berlin D-1000 Berlin 33, F.R.G.*

Received October 10, 1984

Following Fischer's discovery of the first member in 1964, several hundreds of transition-metal carbene complexes have been reported of which, however, few contained more than one carbene ligand per metal atom, and exceedingly few were homoleptic.[2,3] The question arises, whether this reflects an inherent lability of the metal carbene moiety which is overcome by the presence of stabilizing other ligands or, simply, the lack of appropriate synthetic procedures. Undoubtedly, the most promising one in this respect is nucleophilic addition to metal-coordinated isocyanides which, after all, gave the unique tetracarbene palladium and platinum species.[4] There are, however, certain requirements such as the existence of the parent homoleptic isocyanide complexes and a sufficiently high reactivity of all four (or even six) isocyanide ligands, which are barely met.

We wish to demonstrate here that the situation becomes much more favorable if functional isocyanides of the type CNCHRCHR'OH are employed, which contain both the isocyano group and the nucleophile in the same molecule, giving access for the first time to *hexacarbene complexes*.

The reactions between metal chloride and 2-hydroxyalkyl isocyanide were carried out in warm ethanol or water. Air was passed through the solution with the intent of oxidizing cobalt(II) and in anticipation that this would prevent rhodium(III) from being reduced by the isocyanide. Concentration of the solution followed by addition of acetone caused precipitation of **1a–4a** as

white solids (eq 1). Recrystallization from hot alcohol or water
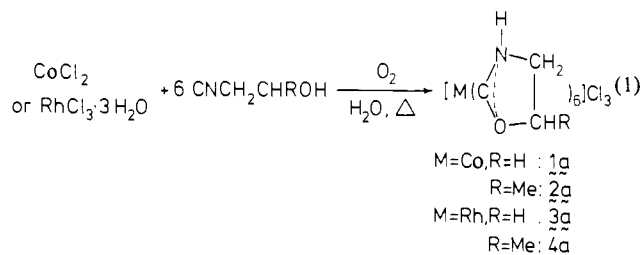
gave clear hexagonal prisms in 75–85% yield which, according to microanalysis, contain varying amounts of water. Drying at 80 °C in vacuo produces hygroscopic but otherwise enormously stable material with decomposition points well above 150 °C.

The molar conductivities of 10^{-7} M aqueous solutions of **1a** and **4a** were found to be 295 and 241 ohm^{-1} cm^2 mol^{-1}, respectively, which is typical of 3:1 electrolytes.[5] Similar properties are shown by the corresponding PF$_6^-$ salts **1b–4b**[6] in acetone and nitromethane solution. With BPh$_4^-$ counterions, on the other hand, a product **1c** was obtained which analyzed as bis(tetraphenylborate) and in fact turned out to be a 1:2 electrolyte in nitromethane (Λ_M(22 °C) = 137 ohm^{-1} cm^2 mol^{-1} at 10^{-7} M). According to solid-state susceptibility measurements, however, **1c** is diamagnetic (χ(293 K) = -1.0×10^6 cgsu), which can only be rationalized by assuming a cobalt(III) species of type **1a** with one of the carbene ligands being deprotonated.

Strong IR absorptions (KBr) at 3400–2900 [ν(NH) + ν(CH)], 1550 [ν_a(Nsb3· ·eb3Csb3· ·eb3O)], and 1160 [ν_s(Nsb3· ·eb3C sb3· ·eb3O)] cm^{-1} as observed in the compounds **1–4** are characteristic of the oxazolidin-2-ylidene ligand as are ^{1}H NMR features in the 7.5–9.5 (NH) and 3.5–4.5 ppm (ring-CH's [AA'BB' resp.ABX multiplets]) regions.[1] More direct support of (terminal) metal–carbon (carbene) bonding in **1–4** comes from the ^{13}C resonances (in D$_2$O or acetone-d_6) at 200–220 ppm and,

(1) Part 2: Fehlhammer, W. P.; Bartel, K.; Plaia, U.; Völkl, A.; Liu, A. T. *Chem. Ber.*, in press.

(2) Fischer, E. O.; Maasböl, A. *Angew. Chem., Int. Ed. Engl.* **1964**, *3*, 580.

(3) Dötz, K. H.; Fischer, H.; Hofmann, P.; Kreissl, F. R.; Schubert, U.; Weiss, K. "Transition Metal Carbene Complexes"; Verlag Chemie: Weinheim, 1983.

(4) Miller, J. S.; Balch, A. L. *Inorg. Chem.* **1972**, *11*, 2069.

(5) Geary, W. J. *Coord. Chem. Rev.* **1971**, *7*, 81.

(6) Typical procedure (**4b**): CNCH$_2$CHMeOH (0.39 mL, 4.56 mmol) was added to a solution of RhCl$_3$·3H$_2$O (0.20 g, 0.76 mmol) in 20 mL of water. After the mixture was warmed to 60 °C, air was bubbled through the mixture for 1 h producing a clear, almost colorless solution to which NH$_4$PF$_6$ (0.37 g, 2.28 mmol) was added with stirring. On cooling to room temperature, analytically pure **4b** separated as white crystals (mp 229–232 °C dec) in almost quantitative yield. Anal. Calcd for C$_{24}$H$_{42}$F$_{18}$N$_6$O$_6$P$_3$Rh: C, 27.50; H, 4.04; N, 8.02. Found: C, 27.78; H, 4.10; N, 8.00.